COMPDYN 2015
5th ECCOMAS Thematic Conference on
Computational Methods in Structural Dynamics and Earthquake Engineering
M. Papadrakakis, V. Papadopoulos, V. Plevris (eds.)
Crete Island, Greece, 25–27 May 2015

OUT-OF-PLANE BEHAVIOUR OF SINGLE-BODY UNREINFORCED-MASONRY WALL RESTRAINED BY A FLEXIBLE DIAPHRAGM

Sanjeev Prajapati[1], **Omar AlShawa**[1], **and Luigi Sorrentino**[1]

[1]Department of Structural and Geotechnics Engineering, Sapienza University of Rome
e-mail: {sanjeev.prajapati, omar.alshawa, luigi.sorrentino } @uniroma1.it

Keywords: : Masonry, out-of-plane, flexible diaphragm, rocking motion.

Abstract. *Past earthquakes have shown the high vulnerability of existing masonry buildings, particularly to out-of-plane local collapse mechanisms. Out-of-plane response is one of the most debated topics in the last decades, because of its complex nature as for geometrical non-linearity, energy damping, record sensitivity. In this work is considered a monolithic wall, resting on a foundation, restrained by a flexible diaphragm. The wall rocks around two base pivots and has one degree of freedom. Its thickness is explicitly accounted for, and the diaphragm is modelled as a linear-elastic spring and a concentrated mass. The non-linear equation of motion is presented, within a lagrangian approach. The energy dissipation is associated to the impact of the wall against the foundation. The effect of size of the wall, diaphragm stiffness and mass are evaluated through parametric analyses. Neglecting the diaphragm mass, the results can be interpreted also as related to a wall restrained at the top by tie-rods.*

1 INTRODUCTION

Earthquakes of the past have shown the great vulnerability of unreinforced-masonry (URM) structures to out-of-plane (OOP) loading (e.g.,[1, 2, 3], and references therein). URM buildings are particularly vulnerable if connections to transversal structures are non-existent or inadequate (e.g., [4], and references therein). However, even if such connections are robust, flexible diaphragms can limit their effectiveness (Fig. 1).

The OOP response of URM connected to a flexible diaphragm has received a comparatively little attention in the past. ABK [5] performed tests on walls acted by two (top and bottom) independent actuators, in order to simulate a possible filter effect of a diaphragm. They suggested stability charts for a mechanism having a base pivot, a top roller and an intermediate hinge. Simsir et al. [6] performed shaking-table tests on a single-storey, single-cell house having a flexible top floor. The authors proposed a single-bar and a two-bars models for replicating the laboratory time histories. Derakhshan [7] proposed an analytical model of a single-storey or a two-storey wall connected to flexible diaphragms. The equations of motion are obtained after a series expansion of trigonometric terms up to second order, with equivalent linear rotational springs simulating the wall-segments response. Penner [8] performed experimental tests on walls having a flexible top restraint and simulated them by means of a commercially-available rigid-body software.

In this paper a wall connected to a flexible restraint will be considered. The restraint can be at any height of the wall, and the thickness of the latter is accounted for. The wall cannot crack along its height, so only a base pivot will be considered. Friction is assumed to be large enough to prevent sliding both at the base and at connection with the diaphragm. A parametric analyses investigates the sensitivity to wall geometry, diaphragm features, ground motion intensity measures.

Figure 1: Out-of-plane damage of a facade segment, L'Aquila (central Italy) 2009.

2 ANALYTICAL MODEL

In the technical literature most of the interest has been so far concentrated on a single rocking body, resting on a foundation, without any top restraint (e.g., [9], and references therein). However, in several cases a masonry wall supports a top horizontal structure. If a tie-rod or a connection to the floor is present, a top restraint can be introduced in the model. Due to this topology, the wall may rotate as a single body or crack along its height. The latter case is typical of slender walls [10], but will not be discussed here. The former case is typical of squatter walls or walls with comparatively small mass with respect to the diaphragm and to the masonry bonding strength [6]. In the following a model of a rocking body, having finite thickness and an horizontal flexible restraint, modelled as a spring, is developed (refer to Fig. 2a). The spring can be in a generic vertical position, not necessarily at the top, but at the centre of the wall thickness in order to preserve vertical symmetry.

2.1 Equation of motion

The analytical equation of motion is derived within a lagrangian approach [11]:

$$\frac{d}{dt}\left(\frac{\partial L}{\partial \dot{\theta}}\right) - \frac{\partial L}{\partial \theta} = Q \tag{1}$$

where:
$L = T - V$; T is the kinetic energy, V is the potential energy, t is the time, $\dot{\theta}$ is the angular velocity, θ is the angular displacement, Q is the non-conservative force.
In the case at hand, the kinetic energy is equal to:

$$T = \frac{1}{2} I_G \dot{\theta}^2 + \frac{1}{2} m \left(\mathbf{v}_{G,A}^2 + \chi \mathbf{v}_{D,A}^2\right)$$

where:
I_G is the moment of inertia of the body about its centre of mass, G (refer to Fig. 2a); m is the mass of the wall; $\chi = m_d/m$; m_d is the mass of the diaphragm; $\mathbf{v}_{G,A}, \mathbf{v}_{D,A}$ are the velocity vectors (refer to Fig. 2c).
Assuming a flat base and neglecting any indentation of the pivot with respect to the geometrical corner of the wall, the potential energy is equal to:

$$V = mg(P_{G,A,y} + \chi P_{D,A,y}) + \frac{1}{2} k_d S_{D,A,x}^2$$

where:
g is the gravity acceleration; $P_{G,A,y}$, $P_{D,A,y}$ are the y-component of position vectors; k_d is the stiffness of the spring; $S_{D,A,x}$ is the x-component of displacement vector (refer to Fig. 2c).
The non-conservative force Q is obtained after derivation of the virtual work W:

$$Q = \frac{dW}{d\theta}$$

The virtual work is obtained as:

$$W = -m\ddot{x}_g \left(S_{G,A,x} + \chi S_{D,A,x}\right) - m\ddot{y}_g \left(S_{G,A,y} + \chi S_{D,A,y}\right)$$

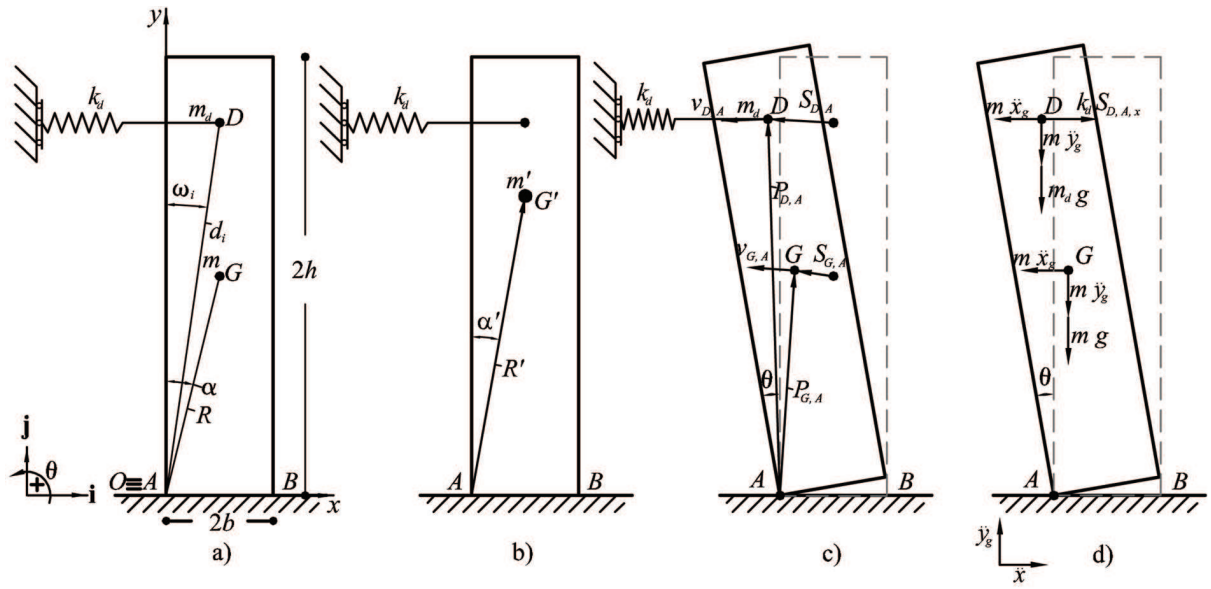

Figure 2: Proposed model: a) Geometric parameters; b) Centre of mass of wall mass + diaphragm mass; c) Position, displacement, and velocity vectors; and d) Conservative and non-conservative forces

where:
$\ddot{x}_g$, $\ddot{y}_g$ are the ground accelerations in x-direction and y-direction, respectively; $S_{D,A,y}$, $S_{G,A,y}$ are the y-component of displacement vectors (refer to Fig. 2c); $S_{G,A,x}$ is the x-component of the displacement vector.

By substituting all the terms in Eq. (1), one can find the following second order non-linear differential equation:

$$\ddot{\theta} \;=\; -p'^2 \left[\frac{\ddot{x}_g}{g} N_1(\alpha', \theta) + \frac{g + \ddot{y}_g}{g} N_2(\alpha', \theta) + \lambda N_3(R', d_i, \omega_i, \theta) \gamma(\theta) \right] \tag{2}$$

where:

$\ddot{\theta} =$ angular acceleration of the body;

$p' = \sqrt{\dfrac{m'R'g}{I'_O}}$, (frequency parameter of the wall [12]);

$m' = m + m_d$;

$R', \alpha' =$ polar coordinates of the centre of mass G' of the system, wall + diaphragm (refer to Fig. 2b);

$d_i, \omega_i =$ polar coordinates of diaphragm connection point D (refer to Fig. 2a);

$I'_O = I_G + m'R'^2$;

$\lambda = \dfrac{k_d R'}{m'g}$;

$\gamma(\theta) =$ fracture function; $\theta_u =$ fracture rotation (refer to Fig.3).

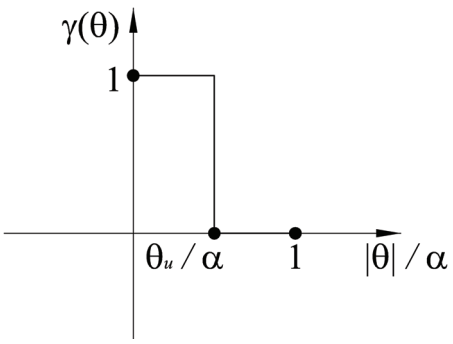

Figure 3: Fracture function of spring

The restraint is assumed as a linear-elastic spring, effective up to a limit displacement related to a limit rotation θ_u. Hence, the spring is active only if the fracture function $\gamma(\theta)$ = 1 (refer to Fig. 3). A qualitatively similar restraint has been considered in [13], where it anchored a block to its foundation. In some of the following analyses an additional condition will be set on the rotation causing the failure of the wall-spring connection. Once this connection has failed the wall will still carry the additional mass but will lose the contribution N_3 in Eq. (2). This condition can be considered representative of a facade losing the contribution of tie-rods. If the failure of the spring is considered as the ultimate limit state, the following plots shall be considered as meaningful up to the limit rotation θ_u/α.

It is possible to emphasise that if m_d = 0 the results can be interpreted as related to a wall restrained by tie-rods. If, additionally, χ = 0, the equation of motion reduces to that by Housner [14].

The condition of minimum ground acceleration for the initiation of motion from rest, when subjected to a base excitation, is given by: $\ddot{x}_g \geqslant \tan\alpha'(g+\ddot{y}_g)$. The condition for overturning is $\theta = \pi/2$. In case of overturning, for the sake of simplification of the following plots, normalised maximum rotation will be set equal to unity.

2.2 Dissipation of energy

Eq. (2) has no damping term. During the rocking motion the block impacts the base and a change of hinge from one corner to the other takes place. A loss of energy is associated to this switch of hinge, through a reduction of velocity after impact. This velocity is derived by assuming the conservation of angular momentum at the instant of impact [14], considering the position of the centre of mass G'. Experimentation on free rocking walls has shown that the analytical coefficient of restitution must be reduced by approximately 5 $\%$ [15]. Although this value was obtained for free-standing walls, it will be assumed also for the case at hand.

The solution of Eq. (2) is obtained through a state-space formulation and a Runge-Kutta method with variable time step in a Matlab environment. The impacts, spring fracture, and overturning are detected through an event strategy.

3 PARAMETRIC ANALYSIS

The derived equation of motion is used to evaluate the effect of wall aspect ratio and size, diaphragm mass, diaphragm stiffness, spring displacement capacity, ground excitation. Based on [10], twelve different aspect ratios are considered, taking $\alpha = [0.025 : 0.025 : 0.300]$ rad. Four values are selected for the size of the wall: $R = [1.5, 3.0, 4.5, 6.0]$ m. Five values of the diaphragm mass / wall mass ratio have been considered: $\chi = [0.00 : 0.05 : 0.20]$. Minimum

No.	Event	Year	Station	Component	PGA	PGV
					g	cm/s
1	Imperial Valley CA, USA,	1940	El Centro Array	40ELC180	0.31	29.80
2	Kern County, CA, USA	1952	Talf Lincoln School	TAFT111	0.18	17.61
3	San Fernando, CA, USA	1971	Pacoima Dam, abutment	PAC164	1.17	114.40
4	Friuli, Italy	1976	Tolmezzo	TOLMEZWE	0.35	32.11
5	Imperial Valley, CA, USA	1979	Site 1	IVC230	0.46	109.26
6	Imperial Valley, CA, USA	1979	Bonds Corner	BCR230	0.78	45.90
7	Irpinia, Italy	1980	Sturno	STURWE	0.31	70.00
8	Irpinia, Italy	1980	Bagnoli Irpino	BAGNIRWE	0.17	37.70
9	Irpinia, Italy	1980	Calitri	CALITWE	0.18	31.72
10	Nahanni, Canada	1985	Site 1	1ST280	1.10	46.10
11	Michoacan,Mexico	1985	Secretaria comunication zone and tran. Texcoco lake bed	SECREN27	0.17	59.81
12	Chile	1985	Llolleo	LLOLLN10	0.71	41.76
13	Landers, CA, USA	1992	Joshua Tree Fire	JOSHUA90	0.28	42.68
14	Northridge, CA, USA	1994	Rinaldi Receiving Station	RRS228	0.84	166.10
15	Northridge, CA, USA	1994	Sylmar-Olive View Med Parking Lot Free Field	SYL360	0.84	129.37
16	Kobe, Japan	1995	KJMA	KJM000	0.82	81.30
17	Kobe, Japan	1995	Takatori	TAK000	0.61	127.10
18	Umbria-Marche	1997	Colfiorito	R1139EW	0.44	24.60
19	ChiChi, Taiwan	1999	TCU129	TCU129W	1.01	59.62
20	Kocaeli, Turkey	1999	Yarimca Petrokimya Tesisleri	YPT330	0.35	62.18
21	L′Aquila, Italy	2009	Val Aterno, Fiume Aterno	AQAX	0.39	30.53
22	L′Aquila, Italy	2009	Val Aterno, Colle Grilli	AQGX	0.42	33.57
23	L′Aquila, Italy	2009	Val Aterno, Aquilparking	AQKY	0.34	38.53
24	L′Aquila, Italy	2009	Val Aterno, Castello	AQUX	0.28	20.91
25	L′Aquila, Italy	2009	Val Aterno, Centro Valle	AQVX	0.63	32.67

Table 1: Acceleration time history records considered. PGA (PGV) = Peak Ground Acceleration (Velocity).

and maximum values of the geometric parameters of the combined system result α' = 0.03, 0.26 rad and R' = 1.50, 6.92 m.

As for diaphragm stiffness, Derakhshan [7] suggested as minimum and maximum values approximately 100 and 5000 kN/m. These values are considered relevant for New Zealand and North American buildings. Consequently, five values of diaphragm stiffness are chosen: $k_d = [0, 100, 500, 1000, 5000]$ kN/m. Displacement capacity of diaphragms is simply varied parametrically, θ_u/α = [0.2 : 0.2 : 1.0]. A much larger maximum value, 10, has been also considered but is not plotted in the following, because delivers results rather similar to θ_u/α = 1.0. It is worth mentioning that Wilson [16] suggested a diaphragm limit displacement equal to 70% of the wall thickness.

Twenty five acceleration natural records have been selected in order to cover a wide range of amplitude, frequency content, distance from the source, magnitude, source mechanism. The accelerograms are mostly the same in [17], with the addition of a few records related to more recent seismic events [18]. Only horizontal components of ground motion are considered. Some basic details of the accelerograms are shown in Table 1.

The total number of analyses computed is equal to 30 000. The response of the wall is plotted as normalised maximum rotation (y-axis), and as a function of α (x-axis) plus one of the parameters previously mentioned.

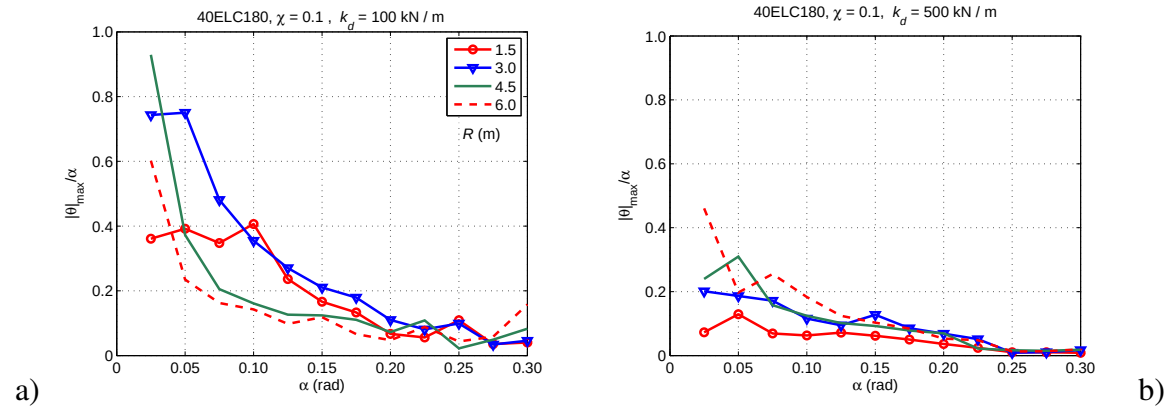

a) b)

Figure 4: Normalised maximum rotation for varying aspect ratio, angle α, and wall size R. Non dimensional diaphragm mass $\chi = 0.10$, Fracture rotation θ_u/α = 1.0, record 40ELC180 (Table 1). Diaphragm stiffness: a) $k_d = 100$ kN/m; b) $k_d = 500$ kN/m.

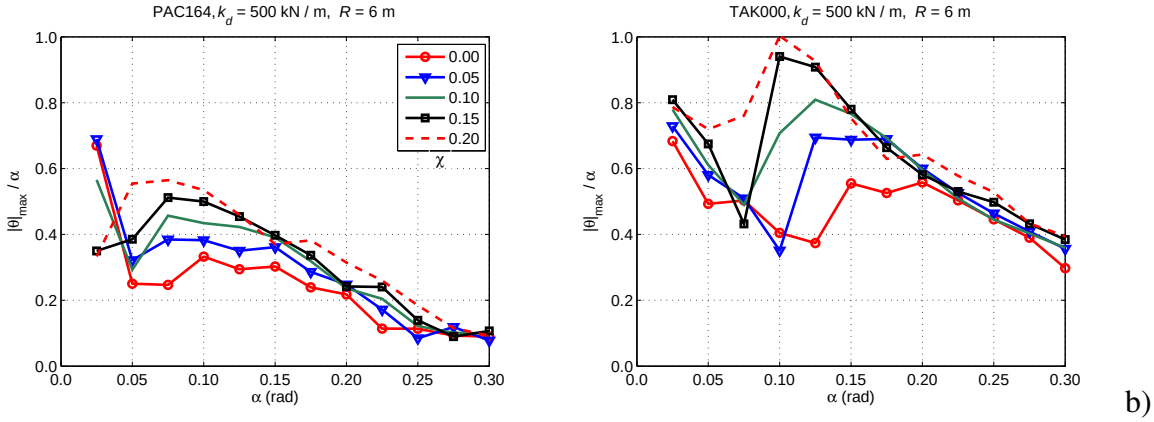

a) b)

Figure 5: Normalised maximum rotation for varying aspect ratio, angle α, and non dimensional diaphragm mass, χ. Size of the wall, R = 6.0 m, Diaphragm stiffness $k_d = 500$ kN/m, Fracture rotation θ_u/α = 1.0. Record: a) PAC164; b) TAK000 (Table 1).

3.1 Effect of wall size

It is well known in the literature that, other things being equal, rocking systems benefit from a larger size [14, 17]. This is the case also here, if the stiffness of the spring is comparatively small (refer to Fig. 4a). However, if the stiffness is increased the role of this so-called ”scale effect” becomes less significant, and actually a ”reversed scale effect” can be observed (refer to Fig. 4b). This appears to be so because the stability of the wall relies more and more on the spring. Nonetheless, the same spring, having constant stiffness, is used for walls of different size and, thus, weight. Consequently, the spring is more effective for small (lighter walls), than for large (heavier) walls.

3.2 Effect of diaphragm mass

The effect of non-dimensional diaphragm mass is investigated in Fig. 5. There it is possible to notice that increasing the floor mass, the response increases. This behaviour can be linked to the increase of the height of the centre of mass of the combined system, making the system more slender through a smaller angle α' (refer to Fig. 2b). This effect, detrimental on stability, is not compensated by the beneficial increase of size, R', associated to the additional floor mass.

3.3 Effect of diaphragm stiffness

In Fig. 6 the stiffness of the diaphragm is varied parametrically. The relevance of this parameter is dramatic, with large values of k_d significantly reducing the maximum rotation. Of course this depends on the assumption of a single-body mechanism. If the spring is that stiff and the connection is adequately robust, a different mechanism (with an intermediate hinge [10]), can be triggered and needs to be assessed. Low values of the stiffness show a less predictable behaviour, and the scattered response typical of rocking systems prevails.

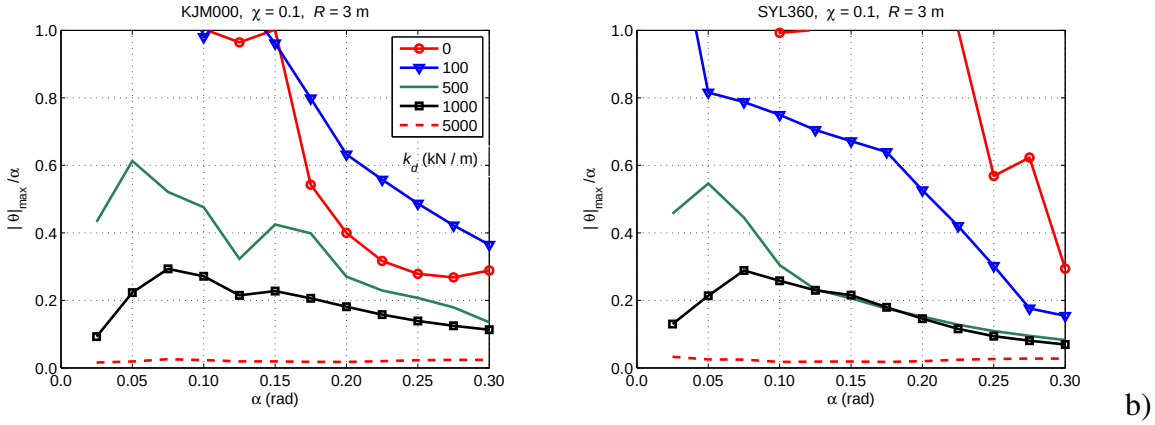

Figure 6: Normalised maximum rotation for varying aspect ratio, angle α, and diaphragm stiffness, k_d. Wall size R = 3.0 m, Non dimensional diaphragm mass $\chi = 0.10$, Fracture rotation θ_u/α = 1.0. Record: a) KJM000; b) SYL360 (Table 1).

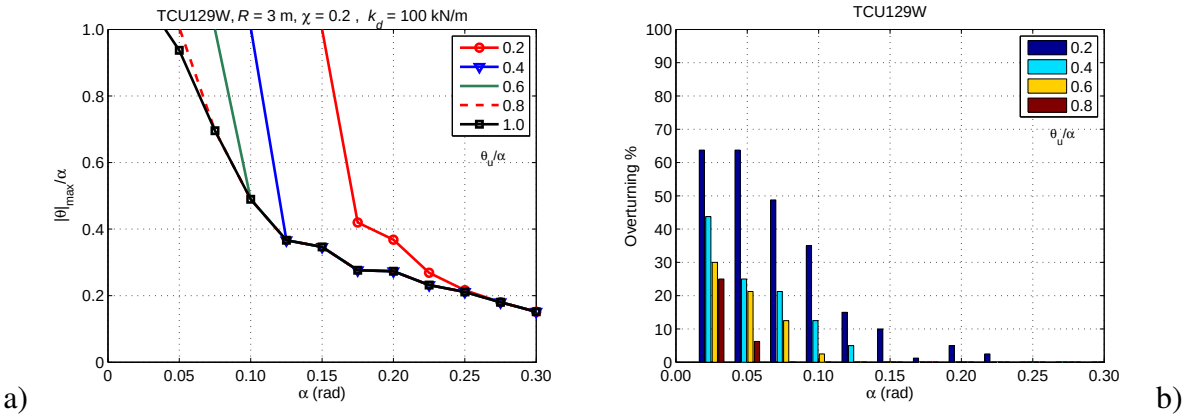

Figure 7: a) Normalised maximum rotation for varying aspect ratio, angle α, and non-dimensional rotation inducing the failure of the spring, θ_u/α. Size of the wall, R = 3.0 m, Non dimensional diaphragm mass χ = 0.2, Diaphragm stiffness $k_d = 500$ kN/m, Record: TCU129 (Table 1). b) Occurrence of overturning, varying non-dimensional fracture rotation, over the entire range of parametric analyses. For θ_y/α = 1.0, no overturning occurs. Record TCU129 (Table 1).

3.4 Effect of displacement capacity of the spring

The role of the displacement capacity of the spring is investigated in Fig. 7. Reducing the fracture rotation will cause an increase in the wall response, because the contribution N_3 in Eq. (2) will be lost. This is evident both in terms of maximum rotation (refer to Fig. 7a) and in

terms of occurrence of overturning (refer to Fig. 7b). The effect is less relevant for large values of α because, in this case, the wall is stable in itself.

3.5 Effect of ground acceleration record

The record-to-record sensitivity is investigated in Fig. 8. There the accelerograms are sorted for descending PGV (Peak Ground Velocity). The response shows an increasing trend for increasing PGV, as already observed in the literature for rocking systems ([19]), but this intensity measure is not sufficient to explain the observed behaviour. Some records (e.g., STURWE,

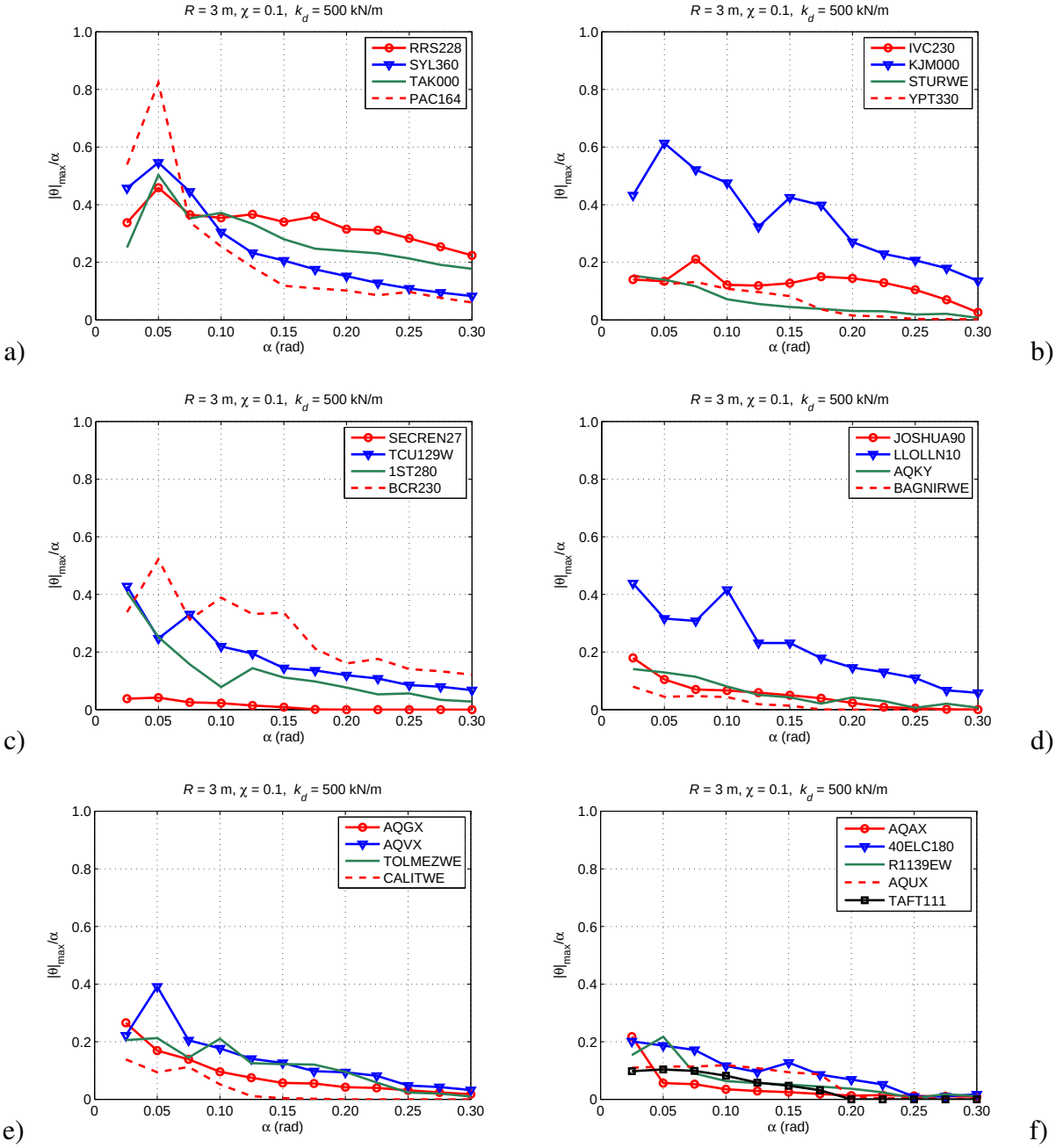

Figure 8: Normalised maximum rotation for varying aspect ratio, angle α, and Record (Table 1). Accelerograms sorted, a)-f), for descending Peak Ground Velocity. Size of the wall R = 3.0 m, Non-dimensional diaphragm mass χ = 0.10, Diaphragm stiffness $k_d = 500$ kN/m, Fracture rotation θ_u/α = 1.0.

YPT330, SECREN27) show a comparatively low maximum amplitude, despite the rather high PGV. In such cases the motion is not activated, or is barely activated, because the minimum acceleration is comparable with the PGA (Peak Ground Acceleration) of the record. The opposite takes place when, for similar PGV, the PGA is rather large (e.g., KJM000, LLOLLN10). Finally, it is possible to notice that an increasing stiffness of the restraint makes the response less scattered.

4 CONCLUSIONS

In this paper the non-linear equation of motion of a single-body wall supporting an additional mass and restrained by an elastic spring has been derived. The wall has a flat base and no indentation at the pivot corners. The spring may represent both a flexible diaphragm and a strengthening intervention through tie-rods.

The equation is used to investigate the sensitivity to a number of parameters. Some of these are related to the wall geometry. The response decreases with a decreasing aspect ratio (height/thickness ratio). Similarly it decreases with an increasing size of the wall. This latter effect is evident if the stiffness of the diaphragm is comparatively low. However, if the stiffness becomes substantial, a ”reversed scale effect” can be observed: the larger the wall the larger the response because the wall is heavier and the spring becomes less effective.

Other parameters are related to the diaphragm. Increasing its mass, compared to the wall, will cause an increase in the maximum rotation, because the centre of mass of the combined system is shifted to the top. The stiffness of the diaphragm is a parameter that dramatically influences the results. High, but still reasonable, values of the stiffness can substantially limit the response. However, in such case, it is necessary to check the robustness of the connections and the activation of a different mechanism, displaying an intermediate hinge. The displacement capacity of the restraint is also significant, because after the premature failure of the spring the stability of the system will rely on its geometry alone.

Record sensitivity is reduced by an increasing spring stiffness. Moreover, the system displays a sensitivity to Peak Ground Velocity, as observed in the literature for other rocking systems. However, this intensity measure is not sufficient to explain completely the observed response. In fact, due to the assumed flat base, sometimes the motion is not activated or it is barely activated.

The study needs to be completed investigating both ground motion characteristics (especially the role of the vertical component), wall characteristics (imperfections and indentations at the base), diaphragm characteristics (position with respect to wall height, displacement capacity and asymmetric - internal-external - behaviour), characteristics of the connection between wall and diaphragm (in order to establish possible dynamic amplifications and the role of an elasto-plastic response), and to consider this mechanism within a wider framework where other mechanisms are also accounted for.

ACKNOWLEDGEMENTS

The authors acknowledge the contribution of the European Commission through a PhD fellowship to the first author within the EU-NICE Erasmus Mundus project [20]. This work has been partially carried out under the program ”Dipartimento della Protezione Civile - Consorzio ReLUIS”, signed on 2013-12-27, Research line Masonry structures. The opinions expressed in this publication are those of the authors and are not necessarily endorsed by the Dipartimento della Protezione Civile.

REFERENCES

[1] M. Bruneau, State-of-the-art report on seismic performance of unreinforced masonry buildings. *Journal of Structural Engineering*, **120**, 230-251, 1994.

[2] L. Sorrentino, L. Liberatore, D. Liberatore, R. Masiani, The behaviour of vernacular buildings in the 2012 Emilia earthquakes. *Bulletin of Earthquake Engineering*, **12**, 2367-2382, 2014. DOI: 10.1007/s10518-013-9455-2.

[3] L. Sorrentino, L. Liberatore, L. D. Decanini, D. Liberatore, The performance of churches in the 2012 Emilia earthquakes. *Bulletin of Earthquake Engineering*, **12**, 2299-2331, 2014. DOI: 10.1007/s10518-013-9519-3.

[4] O. A. Shawa, G. Felice, A. Mauro, L. Sorrentino, Out-of-plane seismic behaviour of rocking masonry walls. *Earthquake Engineering and Structural Dynamics*, **41**, 949-968, 2012. DOI: 10.1002/eqe.1168.

[5] ABK, Joint Venture, *Methodology for mitigation of seismic hazards in existing unreinforced masonry buildings: wall testing, out of plane*. Agbabian Associates:El Segundo, CA, 1981.

[6] C. C. Simsir, M. A. Aschheim, D. P. Abrams, Out-of-plane dynamic response of unreinforced masonry bearing walls attached to flexible diaphragms. *In Proceedings of the 13ˆth World Conference on Earthquake Engineering*, Vancouver, B.C., Canada, August 1-6, 2004.

[7] H. Derakhshan, *Seismic assessment of out of plane loaded unreinforced masonry walls*. ResearchSpace@ Auckland, 2011.

[8] O. Penner, *Out-of-plane dynamic stability of unreinforced masonry walls connected to flexible diaphragms*. The University of British Columbia, Faculty of Graduate and Postdoctoral Studies, 2014.

[9] T. M. Ferreira, A. A. Costa, A. Costa, Analysis of the out-of-plane seismic behaviour of unreinforced masonry: A literature review. *International Journal of Architectural Heritage*, 2014. DOI: 10.1080/15583058.2014.885996.

[10] L. Sorrentino, R. Masiani, M. Griffith, The vertical spanning strip wall as a coupled rocking rigid body assembly. *Structural Engineering and Mechanics*, **29**, 433-453, 2008.

[11] L. Meirovitch, *Elements of vibration analysis, Vol. 2*. New York: McGraw-Hill, 1986.

[12] A. Mauro, G. de Felice, M. J. DeJong, The relative dynamic resilience of masonry collapse mechanisms. *Engineering Structures*, **85**, 182-194, 2015. DOI: 10.1016/j.engstruct.2014.11.021.

[13] N. Makris, J. Zhang, Rocking response of anchored blocks under pulse-type motions. *Journal of Engineering Mechanics*, **127**, 484-493, 2001. DOI: 10.1061/(ASCE)0733-9399(2001)127:5(484).

[14] G. W. Housner, The behavior of inverted pendulum structures during earthquakes. *Bulletin of the seismological society of America*, **53**, 403-417, 1963.

[15] L. Sorrentino, O. AlShawa, L. D. Decanini, The relevance of energy damping in unreinforced masonry rocking mechanisms. Experimental and analytic investigations. *Bulletin of Earthquake Engineering*, **9**, 1617-1642, 2011. DOI: 10.1007/s10518-011-9291-1.

[16] A. W. Wilson, *Seismic assessment of timber floor diaphragms in unreinforced masonry buildings*. Doctoral dissertation, ResearchSpace@ Auckland, 2012.

[17] L. Sorrentino, R. Masiani, L. D. Decanini, Overturning of rocking rigid bodies under transient ground motions. *Structural Engineering and Mechanics*, **22**, 293-310, 2006.

[18] L. Sorrentino, O. Alshawa, D. Liberatore, Observations of Out-of-Plane Rocking in the Oratory of San Giuseppe Dei Minimi during the 2009 L'Aquila Earthquake. *Applied Mechanics and Materials*, London; United Kingdom, June 21-22, 2014. Code 107472. DOI: 10.4028/www.scientific.net/AMM.621.101.

[19] L. Sorrentino, D. DAyala, G. de Felice, M. Griffith, S. Lagomarsino, G. Magenes, Review of out-of-plane seismic assessment techniques applied to existing masonry buildings. *International Journal of Architectural Heritage*, submitted 2015.

[20] M. Faggella, G. Monti, F. Braga, R. Gigliotti, M. Capelli, E. Spacone, M. Laterza, T. Triantafillou, H. Varum, M. Dost Safi, J. Subedi, A. Dixit, S. Lodi, Z. Rahman, S. Limkatanyu, Y. Xiao, L. Yingmin, H. Kumar, W. Salvatore, A. Cecchini, P. Lukkunaprasit, EUNICE, Eurasian University Network for International Cooperation in Earthquakes. *15ˆth World Conference of Earthquake Engineering,(15WCEE)*, Lisboa, Portugal, September 24-28, 2012.